RI URBANS

HORIZON 2020

European Commission

Guidance documents on measurements and modelling of novel air quality pollutants:

Ultrafine particles modelling

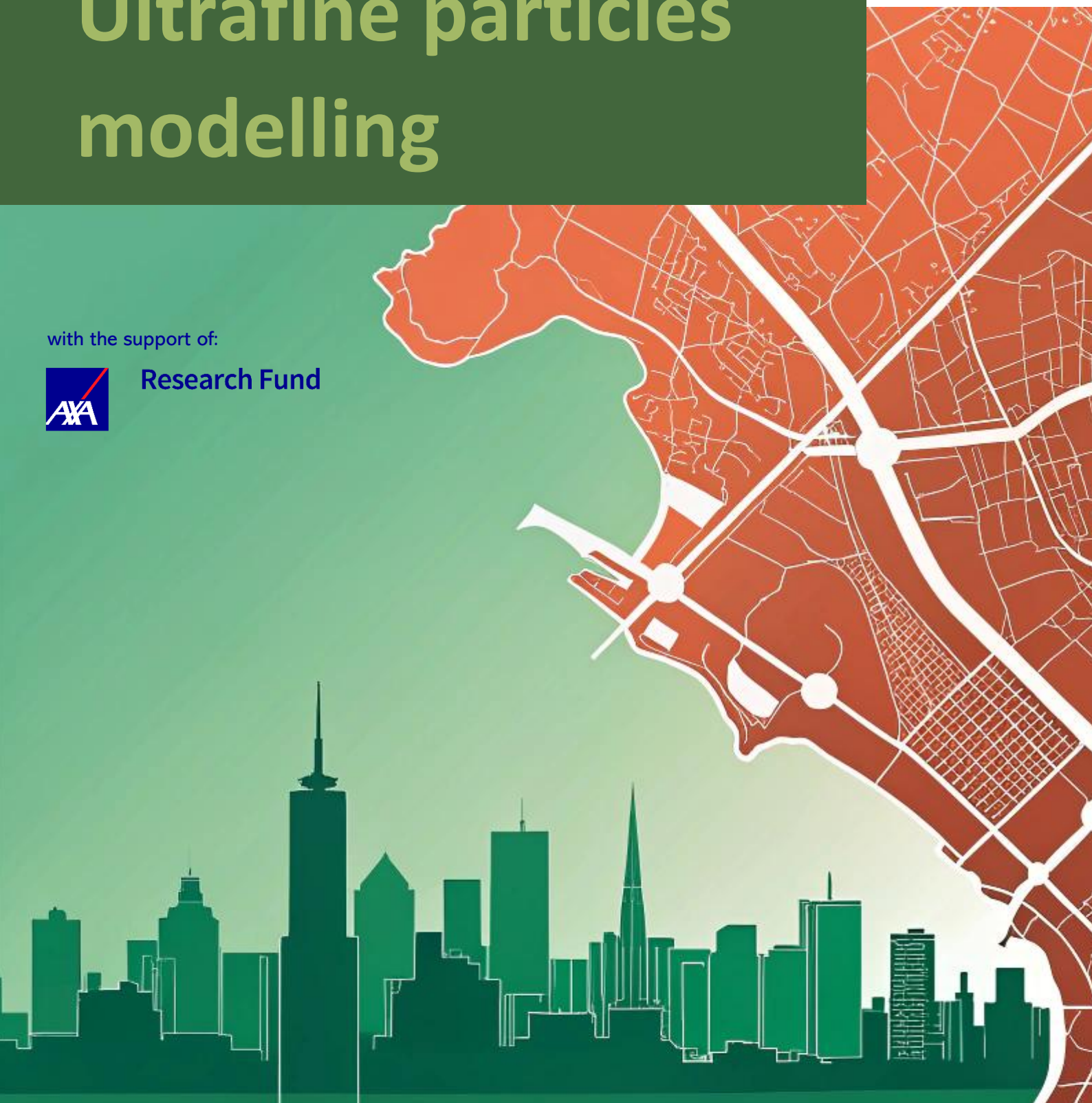

with the support of:

AXA Research Fund

Authors: Evangelia Siouti (FORTH), Karine Sartelet (ENPC), Elena Poulikidi (FORTH), David Patoulias (FORTH), Lya Lugon (ENPC), and Spyros N. Pandis (FORTH)

Reviewed by: Augustin Colette (INERIS), Maria Kanakidou (FORTH), Elli Suhonen (FMI), Martijn Schaap (TNO), Xavier Querol (CSIC)

Cover image created with AI using RECRAFT

Research Infrastructures Services Reinforcing Air Quality Monitoring Capacities in European Urban & Industrial AreaS (RI-URBANS)

RI-URBANS (http://www.RIURBANS.eu) is supported by the European Commission under the Horizon 2020 – Research and Innovation Framework Programme, H2020-GD-2020, Grant Agreement number: 10103624

Table of Contents

Abbreviations

ACTRIS	Aerosols, Clouds and Trace gases Research InfraStructure
ACTRIS - CAIS	ACTRIS Centre for Aerosol in-Situ Measurements
ACTRIS - ECAC	ACTRIS European Center for Aerosol Calibration and Characterization
CAMS	Copernicus Atmosphere Monitoring Service
CHIMERE	Chemical transport model with eulerian approach
DMANx	Dynamic model for aerosol nucleation
eBC	equivalent Black Carbon
ELVOC	Extremely Low Volatility Organic Compounds
EMEP	European Monitoring and Evaluation Programme
IVOC	Intermediate Volatile Organic Compounds
J_{nuc}	Nucleation rate
MUNICH	Model of urban network of intersecting canyons and highways
OA	Organic Aerosols
PM	Particulate Matter
$PM_{0.01}$	Mass concentration of particles < 0.01 µm
$PM_{0.1}$	Mass concentration of particles < 0.1 µm
PM_{1}	Mass concentration of particles < 1 µm
$PM_{2.5}$	Mass concentration of particles < 2.5 µm
PM_{10}	Mass concentration of particles < 10 µm
PMCAMx-UF	Three-dimensional chemical transport model for ultrafine particle size distribution and composition
PN	Particle Number
PNC	Particle Number Concentration
RI-URBANS	Research Infrastructures Services Reinforcing Air Quality Monitoring Capacities in European Urban & Industrial AreaS EU-project
SOA	Secondary Organic Aerosol
SSH	Aerosol model for physio chemical transformation undergone by aerosols in the troposphere
UCM	Urban Canopy Model
UFP	UltraFine Particles
VOC	Volatile Organic Compounds
WHO	World Health Organization
WRF	Weather Research and Forecasting model

Chemical species

CO	Carbon monoxide
NH_3	Ammonia
NO	Nitrogen monoxide
NO_2	Nitrogen dioxide
NO_x	Nitrogen oxides ($NO+NO_2$)
SO_2	Sulphur dioxide
H_2SO_4	Sulfuric acid

1. ABOUT THIS DOCUMENT

This document was prepared as part of the "Research Infrastructures Services Reinforcing Air Quality Monitoring Capacities in European Urban & Industrial AreaS" (RI-URBANS) EU-project that connects the atmospheric observation expertise from Aerosols, Clouds and Trace gases Research InfraStructure (ACTRIS) as well as the urban air quality observation capacities of the regulatory air quality monitoring networks.

One of the objectives of RI-URBANS is to model concentrations of ultrafine particles (UFP, used as equivalent to nanoparticles or those particles <100 nm). Because >80% of the total particle concentrations (PNCs) falls in the range of UFP (Trechera et al., 2023), UFP is sometimes used as a surrogate of PNC, and vice versa.

UFP can be primary (emitted directly as aerosols to the atmosphere) or secondary (newly formed from nucleation episodes into the atmosphere). In urban áreas both types of ultrafine particles co-exist. Road traffic emissions are often responsable for most of the primary UFPs (Hopke et al., 2022).

To dequately model the spatial-temporal variation of UFP (and their particle number size distribution, PNSD), primary UFP-PNSD emission inventories are required (see ST15 on the first UFP-PNSD EU emission inventory), but also descriptions of complex physical-chemical processes including coagulation, mass transfer of semi and low-volatility chemical compounds between the gas and particulate phases and nucleation processes should be implemented in the modelling tools. Multiscale approaches are also needed to account for the often-significant regional sources and processes with the urban UFP-PNSD. This document summarises methodologies for multiscale modelling of UFP.

This is RI-URBANS a document that summarises methodologies for this specific service tool (STs) that is part of the RI-URBANS deliverable D46 (D6.1, containing guidance for all service tools provided in the project) with the support for publication from AXA Research Fund to build up the final dissemination D55 (D7.6). Any dissemination of results must indicate that it reflects only the author's view and that the European Commission is not responsible for any use that may be made of the information it contains.

2. OVERVIEW OF THE MODELS

PMCAMx-UF: PMCAMx-UF is a three-dimensional chemical transport model that simulates both the number size distribution and the mass/composition distribution of the multicomponent atmospheric aerosol (Jung et al., 2010). This three-dimensional chemical transport model simulates the processes of (natural) emissions, horizontal and vertical advection, horizontal and vertical dispersion, wet and dry deposition, and gas, cloud and aerosol-phase chemistry (Fountoukis et al., 2012). The simulation of the aerosol microphysics is handled by the updated version of the Dynamic Model for Aerosol Nucleation (DMANx), which includes the processes of condensation, evaporation, nucleation, and coagulation assuming an internally mixed aerosol (Patoulias et al., 2015). DMANx includes the TwO-Moment Aerosol Sectional (TOMAS) algorithm, which tracks both mass and number concentrations simultaneously and can use the desired nucleation theory to simulate particles starting from nuclei sizes. The aerosol size distribution is described with 41 size sections starting from 0.8 nm diameter (Jung et al., 2006). The rate of nucleation, J_{nuc}, in DMANx is calculated using two different parameterizations. When the NH_3 concentration is greater than 0.01 ppt, the ternary nucleation parameterization by Napari et al. (2002) is utilized, where nucleation rates depend on H_2SO_4 and NH_3 concentrations, temperature and relative humidity. Conversely, when the NH_3 concentration is below this threshold value, the binary parameterization by Vehkamaki et al. (2002) is employed, where the nucleation rate is a function of H_2SO_4 concentration, temperature, and relative humidity. In sulfur-rich settings, the original NH_3-H_2SO_4-H_2O parameterization had been effective in determining the existence or absence of nucleation events (Gaydos et al., 2005). However, it overestimated ultrafine number concentrations during nucleation events (Fountoukis et al., 2012; Jung et al., 2008, 2010), hence a scaling factor of 10^{-6} is used for the calculation of nucleation rate according to the suggestion of Fountoukis et al. (2012). This is used as the default approach, but a variety of other nucleation rate expressions can be adopted by the user. Adopting the Pierce and Adams (2009) approach, the pseudo-steady-state approach (PSSA) for sulfuric acid is employed. It is assumed that the concentration of sulfuric acid achieves steady state instantly throughout a time step, there is the possibility of computing the nucleation and condensation rates concurrently. Organic compounds can be oxidized in the atmosphere to form secondary organic aerosol (SOA). The volatility basis set (VBS) framework is employed to model the volatility distribution of OA (Patoulias and Pandis, 2022). The formation of SOA is simulated using a second-order process involving the hydroxyl

radical. The aging of IVOCs is modeled using a rate constant k (298 K)=40 × 10^{-12} cm^3 $molecule^{-1}$ s^{-1} (Patoulias and Pandis, 2022). ELVOCS are assumed to be produced by the oxidation of monoterpenes, by reaction with hydroxyl radicals, with a molar yield of 5% (Patoulias and Pandis, 2022).

CHIMERE/MUNICH/SSH-aerosol multi-scale air-quality model chain: CHIMERE/MUNICH/SSH-aerosol is a multi-scale model chain designed to represent regulated and emerging pollutant concentrations from the urban background to the street level (Park et al., 2024). In the regional scale, concentrations are computed using the chemical transport model CHIMERE model v2020r3 (Menut et al., 2021), which is capable to represent the main phenomena related to pollutant dispersion, such as horizontal and vertical advection by the wind (Van Leer, 1977), dry and wet deposition (Wesely, 1967). Gas-phase chemistry is represented using the Melchior2 chemical mechanism (Derognat et al., 2003; Carter, 1990), modified to represent the formation of condensables (Sartelet et al. 2020). CHIMERE v2020r3 is coupled with the WRF model version 3.7.1, which is used to compute the meteorological fields (Skamarock et al., 2008). Urban background concentrations and meteorological fields computed in the regional scale by CHIMERE are then used as boundary conditions by the MUNICH model (Kim et al., 2022) in order to represent concentrations at the street-level. A crucial strength of this multi-scale modelling chain is the coherent representation of gas-phase chemistry and aerosol dynamics at both urban regional and local street scales. Both CHIMERE and MUNICH models are coupled with the 0D chemical module SSH-aerosol (Sartelet et al., 2020), which includes the state-of-art representations of aerosol dynamics, such as condensation/evaporation, coagulation and nucleation. The size distribution is discretized into sections and internal mixing of particles is assumed in the 3D simulations. With the CHIMERE/MUNICH/SSH-aerosol chain, the user can define different levels of complexity to represent aerosol dynamics. For computational efficiency, thermodynamic equilibrium may be assumed for the gas-particle partitioning in condensation/evaporation of organic and inorganic compounds at the regional scale. Secondary organic aerosols are modelled with the surrogate approach (Couvidat and Sartelet, 2015), allowing to consider the hydrophilic and hydrophobic properties of organic compounds. To accurately represent the growth of ultrafine particles, which are evolving fast, nucleation, coagulation, condensation of sulfuric acid and ELVOC are solved together. As a Lagragian approach is used to model condensation/evaporation, the bounds of the particle size sections evolve, and it is necessary to redistribute the number and mass on fixed section bounds. Although different algorithms of redistribution are available in SSH-aerosol, the

Euler-coupled one (Devilliers et al, 2013) is recommended for use within CHIMERE and MUNICH. Different parameterisations of nucleation are implemented: the binary parameterisation of Kuang et al. (2008) involving sulfuric acid and wáter. The nucleation parameterisations may be rescaled (Sartelet et al. 2022). The number of size sections can be setup by the user, as the range of diameters (from 1 nanometer to tens of micrometres). To gain CPU time, nucleation is ignored here, and only particles of diameters larger than 10 nm are modelled. Although in Sartelet et al. (2022), the concentrations simulated with nucleation led to better statistical indicators compared to observations than those simulated without nucleation, the statistical indicators of the concentrations simulated without nucleation are very good. Modelling nucleation implies representing nanoparticles between 1 nm and 10 nm, and hence additional sections between 1 nm and 10 nm are needed to model their dynamics (at least, 4 size sections following Jacquot and Sartelet, 2024). Here, the configuration of the CHIMERE/MUNICH/SSH-aerosol chain uses 10 size sections, from 10 nanometers to 10 micrometres. Ignoring nucleation and having only 10 size sections above 10 nm allows the CPU time to be the same as often used for 3D modelling of $PM_{2.5}$. This configuration was used over Europe and over the city of Paris, representing well particle mass and number in both urban background and streets (Park et al., 2024). This version focuses on primary particles.

2.1 Use of multiple scales

To be able to simulate concentrations with a high spatial resolution (e.g., 1x1 km^2), nested simulations should be performed.

2.1.1 PMCAMx-UF

The ability of PMCAMx-UF to use multiple grids has been used to allow it to focus on specific RI-URBANS pilot cities as a pilot study. The particle number distribution over three cities (Athens, Greece; Barcelona, Spain, and Paris, France) has been simulated for the summer (July) and winter (January) of 2019. PMCAMx-UF is implemented for Europe using three nested grids with increasing spatial resolution focusing on the interested area (e.g. Athens). Constant and relatively low values have been utilized for the boundary conditions of the European domain. The horizontal spatial resolution of the outer European domain is 36×36 km^2, whereas the simulated city has a resolution of 1×1 km^2 (Figure 1). For numerical purposes, the grid size is reduced gradually, so there is an area in which 12×12 km^2 grid cells are used and another with 3×3 km^2. A region of 5400×5832 km^2 is covered by the European domain, while areas of

216×216, 144×144, and 72×72 km^2 are covered by the three nested domains, respectively. Similar grid systems have been used for Paris and Barcelona. Two-way nesting is used for the simulations.

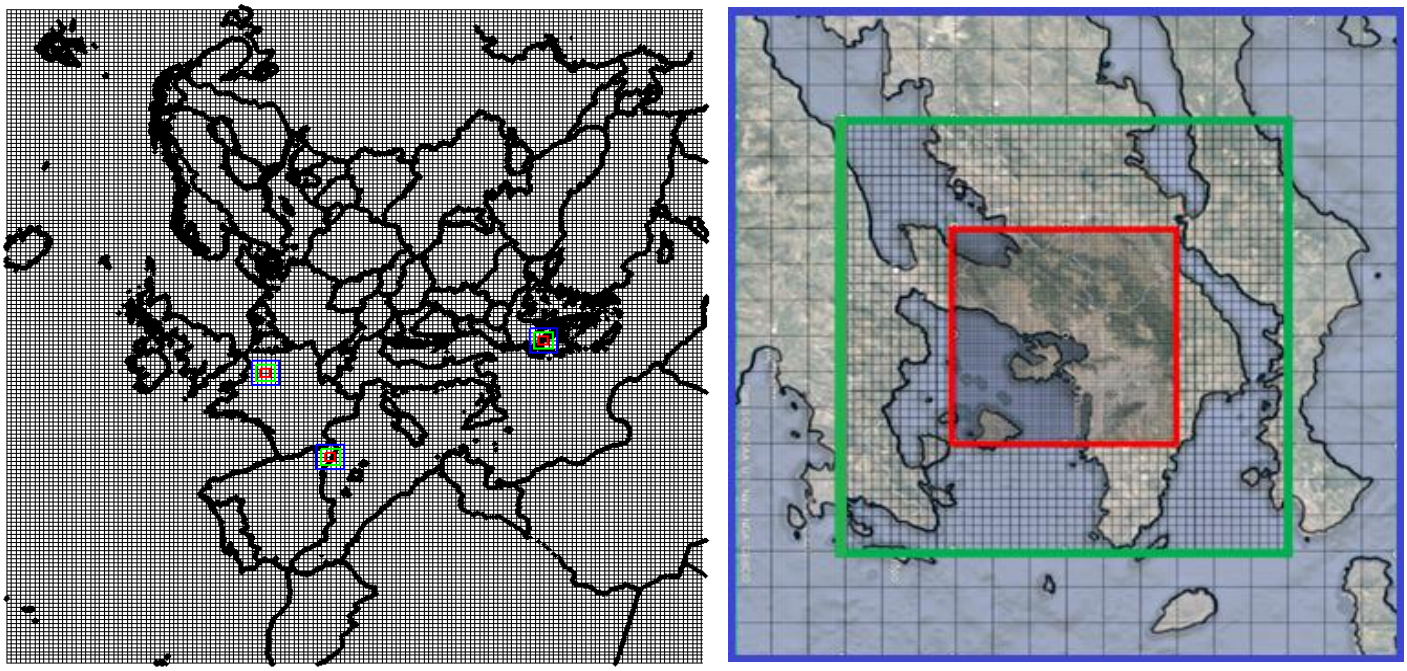

Figure 1. *Example of the multiple modeling scales used in PMCAMx-UF for the pilot city of Athens. (a) The outer European domain (d01) of 36×36 km^2 spatial resolution and (b) the three nested domains with increasing spatial resolution. Blue (d02): 12×12 km^2 spatial resolution, green (d03): 3×3 km^2 and red (d04): 1×1 km^2.*

2.1.2 CHIMERE/MUNICH/SSH-aerosol multi-scale air-quality model chain

In the CHIMERE/MUNICH/SSH-aerosol chain, nested domains are considered using CAMS boundary conditions over the largest domain. An example is provided in Figure 2 for the RI-URBANS pilot city Paris. The smallest domain of CHIMERE simulation is discretized with a 1x1 km^2 resolution (indicated in Figure 2 as d03, in green). A zoom is then performed in the streets of Paris, which are explicitly represented using an eulerian approach with the street network MUNICH. Using a Eulerian approach at the street scale leads to a direct exchange between the background and the street, making it possible to accurately estimate the formation of secondary pollutants. One-way coupling between the urban background (CHIMERE) and the streets (MUNICH) is used here. MUNICH only models the street concentrations. It uses background concentrations above the streets as boundary conditions. These background conditions include contributions from all sources. For streets, only the sources emitted in the streets are included (e.g., traffic, trees) (Maison et al. 2024).

CHIMERE/SSH-aerosol may also be used at the regional scale as a stand-alone model to simulate the concentrations of particles and ultrafine particles. An example of a simulation domain over western Europe is provided in Figure 3, using CAMS boundary conditions over Europe and a 15x15 km^2 spatial resolution. A simulation was performed for 1 May to 31 July 2019 for comparisons to RI-URBANS measurements.

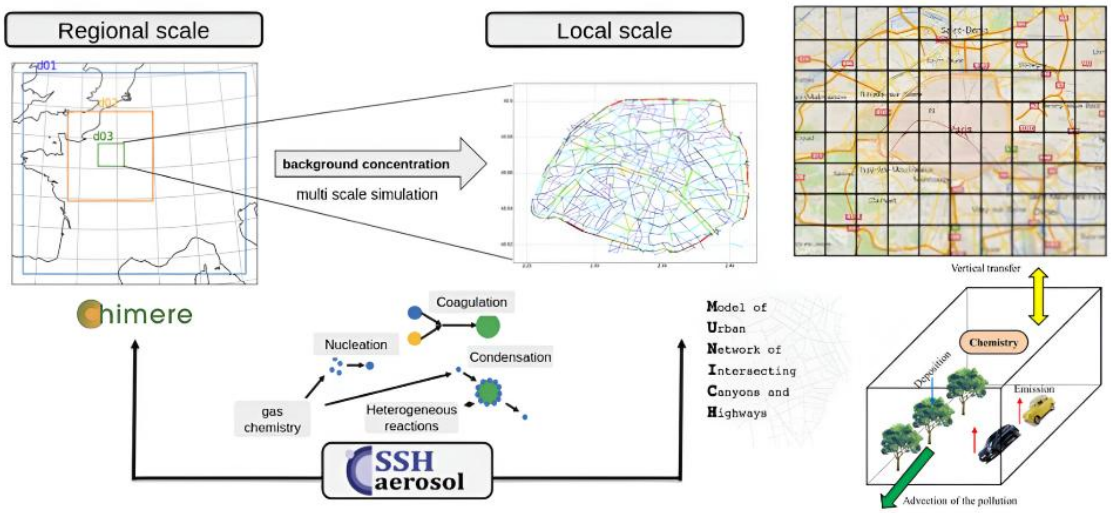

Figure 2. *Example of the multiple modeling scales used in CHIMERE/MUNICH/SSH-aerosol for Paris. (a) The outer European domain (d01) of 9×9 km^2 spatial resolution and (b) the three nested domains with increasing spatial resolution. Orange (d02): 3×3 km^2, green (d03): 1×1 km^2. The street network for Paris city is embedded in the d03 domain, with a street-level resolution.*

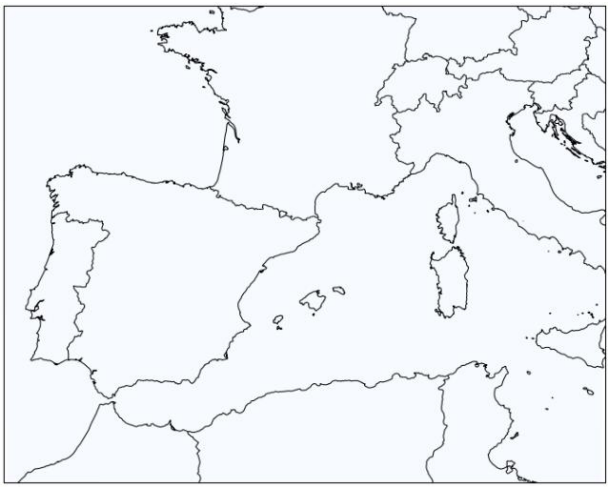

Figure 3. *Example of a simulation domain over Europe simulated using CHIMERE/SSH-aerosol with of 15×15 km^2 spatial resolution.*

2.2 Code availability

- The PMCAMx-UF code is available in the following link: https://zenodo.org/records/10078189.
- The CHIMERE/MUNICH/SSH-aerosol code is available in the following link: https://zenodo.org/records/12639507.

3. INPUT PREPARATION

3.1 Meteorology

In both PMCAMx-UF and CHIMERE/MUNICH/SSH-aerosol, meteorological data are produced using the Weather Research and Forecasting (WRF) mesoscale numerical weather prediction model (Skamarock et al., 2021). Each layer of the chemical transport model is aligned with the layers used in WRF.

3.1.1 PMCAMx-UF

The meteorological fields are downscaled using four two-way nests from the coarse domain (d01) covering Europe at 36×36 km^2 horizontal spatial resolution to the 1×1 km^2 resolution domain over the city (d04) (Figure 1). The d04 is surrounded by the intermediate domains d02 and d03, which have spatial resolutions of 12×12 and 3×3 km^2, respectively. We modelled each city separately.

Global Forecast System (GFS) is used to determine initial and lateral boundary conditions of WRF. WRF receives its topography and land-use geographical datasets from the United States Geological Survey (USGS).

3.1.2 CHIMERE/MUNICH-SSH-aerosol

The meteorological fields are computed by WRF with a one-way nesting over the WRF simulations are performed with 33 vertical levels, from 0 to 20 km altitude. For simulations over the smallest domain, over cities, a more refined vertical discretization is employed in the first four vertical levels, which contains almost all buildings. The land-use dataset employed is CORINE land-use coverage, with a 250 m resolution (available inhttps://doi.org/ 10.2909/71c95a07-e296-44fc-b22b-415f42acfdf0).

In order to represent more precisely the meteorological fields in urban areas, and allow downscaling down to the street scale, the single-layer urban canopy model (UCM) (Kusaka et al., 2001) should be used over

the smallest domain. Three urban categories are employed to differentiate street and building dimensions, as well as heat transfer parameters in commercial, high and low intensity residential areas.

3.2 Anthropogenic emissions

Emission inventories from the different anthropogenic activity sectors are necessary to perform the simulation. PMCAMx-UF is used with the RI-URBANS number emission inventory developed by TNO, whereas CHIMERE/MUNICH/SSH-aerosol is used with either bottom-up or top-down inventories using the methodology presented in Sartelet et al. (2022) and Park et al. (2024) to estimate number emissions from mass-based emissions.

3.2.1 PMCAMx-UF RI-URBANS emission inventory

The RI-URBANS number emission inventory developed by TNO is used for anthropogenic emissions including both area and point emissions (Kuenen et al., 2022). The number/mass emission inventory incorporates both number emissions and consistent size-resolved composition for particles over the size range of approximately 10 nm to 10 µm (30 sizes bins). Sources of anthropogenic emissions include public power, industry, domestic combustion, fugitives, solvents, road transport, non-road transport, shipping, aviation, waste treatment, livestock and agriculture waste burning. Road transport is further subdivided into road transport from exhaust and non-exhaust types, while road transport from exhaust is further split to gasoline, diesel and LPG gas.

All the major air pollutants are included in the emission inventory: SO_2, NO_x, VOCs, NH_3, CO, $PM_{2.5}$, and PM_{10}, as well as UFP, expressed as PN emissions (including parameterized size distributions, currently using the 15 different size bins according to the PMCAMx-UF CTM). The PN inventory covers the size range from 10 to 325 nm (in electrical equivalent mobility) and includes total particles (sum of solid and volatile). Elements such as organic and elemental carbon, sulfate, salt, and other minerals are the chemical composition of particles. Alcohols, monoterpenes, aromatics, alkanals, ketones, and acids are examples of volatile organic molecules that are included in the emission inventory.

The original TNO emissions are prepared in a horizontal spatial resolution of 0.1×0.05 degrees of latitude-longitude), which is equivalent to roughly 6×6 km^2 over central Europe, while the area emissions for the European domain are generated at a spatial resolution of 36×36 km^2 following the PMCAMx-UF grid. High resolution 1×1 km^2 emission inventories were derived for the pilot cities based on this dataset using the

downscaling methodology tool developed by National Observatory of Athens (NOA) (Ramacher et al., 2021) (https://riurbans.eu/wp-content/uploads/2022/07/RI-URBANS_D17_D3.2.pdf). Emissions for d02 and d03 are not used in the current application and PMCAMx-UF does interpolation.

Downscaling: The anthropogenic emissions from the European CAMS-REG emission inventory were downscaled from 0.1°×0.05° (or ~6×6 km^2) to 1×1 km^2 resolution using the NOA downscaling algorithm developed in this project. The improvement is mainly based on a spatial disaggregation approach to provide an increasing accuracy of the annual, anthropogenic emissions over the pilot cities. Publicly accessible, generic, contemporary and high-resolution (≤1×1 km^2) geographical datasets of the European region serve as the basis for the spatial disaggregation of CAMS-REG. These datasets are then converted into sector-specific spatial proxies and applied to the source categories of CAMS-REG. The method is integrated into a fully automated tool that will provide the detailed mapping of all the project's pilot cities' emission sources, including residential, agricultural, and other (area, at the spatial analysis of 1×1 km^2), industrial (point or at the spatial analysis of 1×1 km^2), and transportation (line or at the spatial analysis of 1×1 km^2).

3.2.2 Bottom-up or top-down emission inventory with estimation of number emissions from mass

Number emissions and the size distribution at emissions were estimated from the emission inventory using the methodology detailed in Sartelet et al. (2022) and Park et al. (2024). The emission inventories provide estimations of $PM_{2.5}$ emissions for the different activity sectors. To distribute $PM_{2.5}$ emissions in the modelled particle size sections, first emissions of particles in the range $PM_{0.1}$-PM_1 and $PM_{0.01}$-$PM_{0.1}$ are estimated using the $PM_1/PM_{2.5}$ and $PM_{0.1}/PM_1$ ratios given in Sartelet et al. (2022) for each activity sector. The emissions in each of the size ranges: $PM_{0.01}$-$PM_{0.1}$, $PM_{0.1}$-PM_1, and PM_1-$PM_{2.5}$ are distributed amongst the model size sections with an algorithm that conserves mass and number (Park et al. 2024). Note that for the residential sector, the lowest diameter considers for emission is 80 nm (against 10 nm for the other sectors).

Bottom-up emission inventories may be provided with a 1x1 km^2 spatial resolution. Emission inventories using top-down emission inventories are available at the European scale (e.g. EMEP, CAMS), and they may be downscaled to the city scale down to 1x1 km^2 spatial resolution. A tool for this purpose is embedded in chemistry-transport models (e.g. CHIMERE, Menut et al. 2021), or the methodology defined in the

service tool “EMISSION INVENTORIES FOR REGIONAL AND URBAN SCALE MODELLING APPLICATIONS” may be used. For muti-scale simulations down to the street-scale, hourly road-network emissions are also needed, as detailed in the service tool “DETERMINISTIC URBAN MODELLING: PM & PN”.

3.3 Biogenic emissions

Biogenic emissions are produced using the Model of Emissions of Gases and Aerosols from Nature (MEGAN v3 in PMCAMx-UF and MEGAN v2.1 in CHIMERE) (Guenter et al., 2006; 2012). In PMCAMx-UF, estimated emissions of 201 individual gas-phase chemicals, such as isoprene, monoterpenes, sesquiterpenes, are then combined into 27 simulated species including alkanes, olefins, aromatics, nitrogen dioxide, nitrogen monoxide, ammonia, carbon monoxide, ethene, methane, methanol, acetone, acetaldehyde, formaldehyde, benzaldehyde, higher aldehydes, methylethyl ketone, formic acid, acetic acid, pyruvic acid and methyl acetate. The environmental conditions (temperature, soil moisture, light, wind speed, and humidity) predicted by WRF and land cover data, such as Leaf Area Index (spatial and temporal distribution of canopy growth) and Plant Functional Type distributions, are the driving factors for producing biogenic emissions (Guenter et al., 2006). An activity factor that takes environmental change into account is used in MEGAN to scale the emission under standard settings (Guenter et al., 2012).

3.4 Marine emissions

3.4.1 PMCAMx-UF

Sea-spray aerosol emissions are produced based on O’Dowd et al. (2008) and Monahan (1986) distributions. Organic aerosol and sodium chloride are the main components of sea-spray aerosols. The O’Dowd distribution is used for particles with a diameter lower than 1 µm, whereas the Monahan distribution for particles with a diameter larger than 1 µm. Chlorophyll-a concentrations are required to produce sea-spay aerosol emissions that are obtained from MODIS (Moderate Resolution Imaging Spectroradiometer). Additionally, wind speeds at 22 and 10 m above the sea level, which is produced by WRF, are essential for marine emission model.

3.4.2 CHIMERE/MUNICH/SSH-aerosol

Sea salt emissions in CHIMERE can be computed in function of particle radius and 10m-wind speed based on different approaches, such as Monahan (1986), Matterssoon et al., (2003), Spada et al. (2013) and Grythe et al., (2014) to estimate emission of sodium, chloride and dimethyl sulfide. In the standard

configuration of CHIMERE/MUNICH/SSH-aerosol model chain, the 10m-wind is computed over each domain cell using the WRF model, and sea salt emissions are computed with the Matterssoon et al., (2003) parametrization. This parametrization includes a specific size distribution in the Monahan's scheme, ranging from 0.020 to 2.8 μm. Although forest fire emissions may be included in the modelling with CHIMERE (Menut et al. 2023), they are not included in the application discussed here.

4. OUTPUTS

This section examines the output generated by the models to demonstrate their capabilities.

4.1 PMCAMx-UF

Figure 4 displays the number of concentration of particles with a diameter larger than 10 nm against time in Demokritos for July 2019. The timeseries is especially useful when comparing the predictions of the model with measurements (such a comparison is shown in Figures 14 and 15).

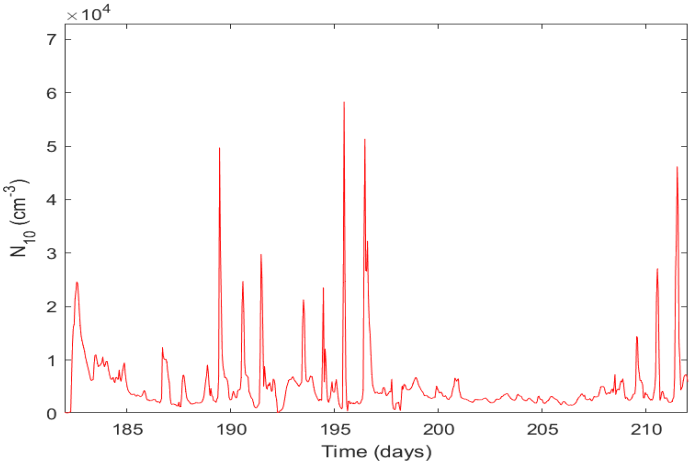

Figure 4. *The predicted number concentration of particles with a diameter larger than 10 nm against time (days) in Demokritos for July 2019*

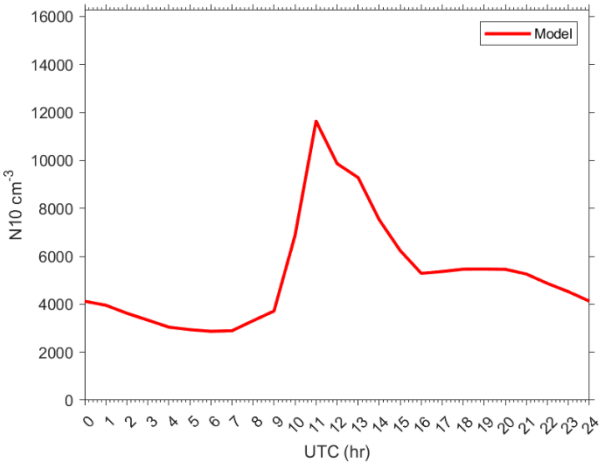

Figure 5. *The average daily profile of N_{10} concentration in Demokritos for July 2019. Thime is standard local time.*

Figure 5 demonstrates the predicted average N_{10} concentration of July 2019 in Demokritos against time (hour). The concentration peaks in the morning hours, when there is plenty of sunlight and emissions from cars.

Figure 6 displays the size distribution of particle number for July 8, 2019, in Athens. Here is a nice example of what a new particle formation day looks like. The predicted aerosol number distribution shows a new distinct mode of particles from 9:00 to 12:00 under 25 nm being formed and undergoing growth.

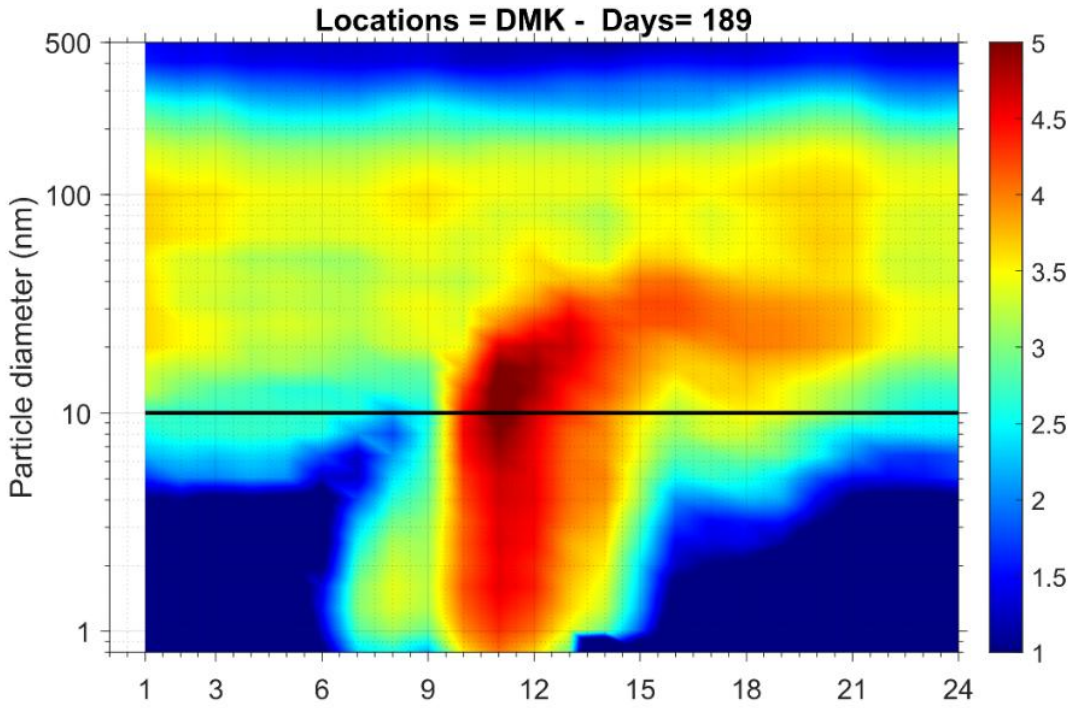

Figure 6. *The predicted size distribution on July 08, 2019, as function of local time at Athens. The particle number distribution (z-axis) is plotted against time of day (x-axis) and particle diameter (y-axis). The x-axis is local standard time and the primary y-axis is particle number distribution is in logarithmic scale, and the colosr of the secondary y-axis are particle number concentrations in #*10^{3} cm^{-3}.*

Figure 7 demonstrates the predicted average number concentration of particles above 10 nm (N_{10}) for July 2019 in (a) Europe and (b) Athens. The capability of the model to use multiple grids allows for much more information to be acquired. In the following figure, high particle concentrations in Europe are predicted over Central Europe and the Mediterranean region. Focusing on Athens, high particle concentrations are predicted over Piraeus port and the Saronic Gulf.

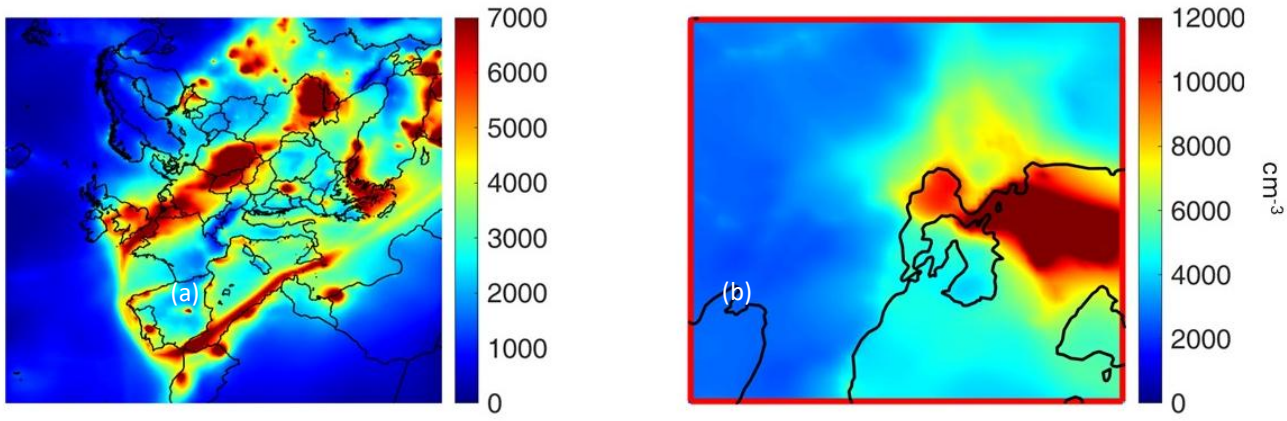

Figure 7. *Predicted average N_{10} concentration for July 2019 over (a) Europe and (b) Athens.*

4.2 CHIMERE/MUNICH/SSH-aerosol

The representation of fine and ultra-fine particles with the chain CHIMERE/MUNICH/SSH-aerosol can be employed (*i*) in multi-scale simulations from the urban background to the street scale, but also in (*ii*) regional-scale simulations, with CHIMERE/SSH-aerosol employed as a stand-alone model. In this last case, Figure 8 illustrates the average N_{10} concentrations computed with CHIMERE/SSH-aerosol over southern western Europe with 15x15 km^2 spatial resolution from May to July 2019. Highest concentrations are observed in dense urban areas, such as Barcelona, Madrid, Algiers and north of Italy.

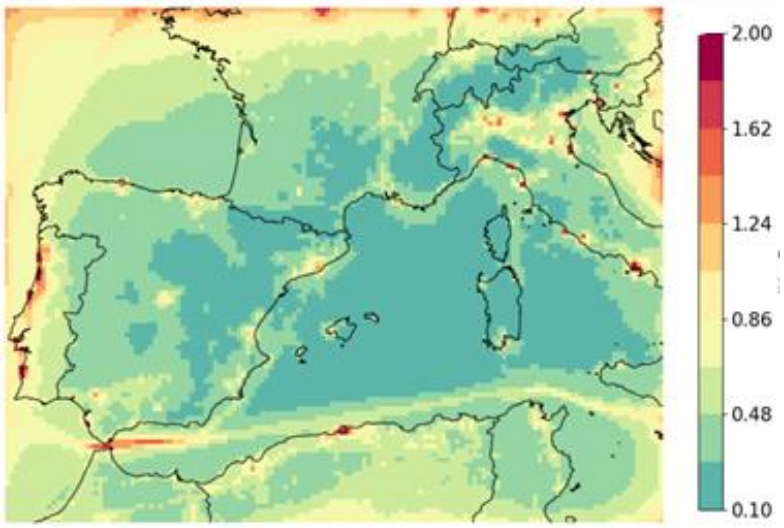

Figure 8. *Predicted average N_{10} concentration for July 2019 over Europe [in 10^4*cm^{-3}].*

Even though the horizontal resolution is coarse, CHIMERE/SSH-aerosol represents well the observed NO_2 and $PM_{2.5}$ concentrations at observation stations available in Spain (Barcelona and Madrid) and Italy (Ispra). At those stations, the total N_{10} concentration and the number distribution per size sections also compare well to observations, as illustrated in Figures 9, 10 and 11, respectively.

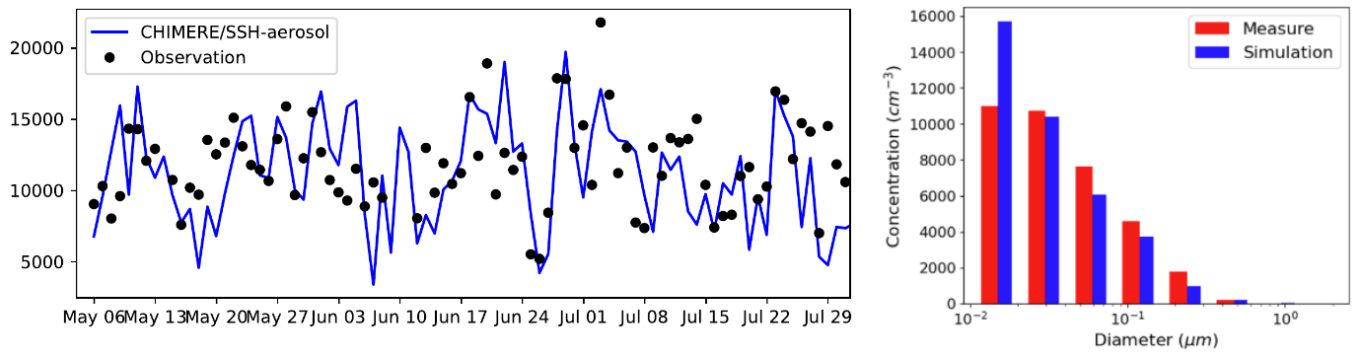

Figure 9. *Model to data comparison of N_{10} concentrations simulated over Barcelona, Spain. The left panel illustrates the total N_{10} temporal evolution and the right panel the number concentration per size section [in cm^{-3}].*

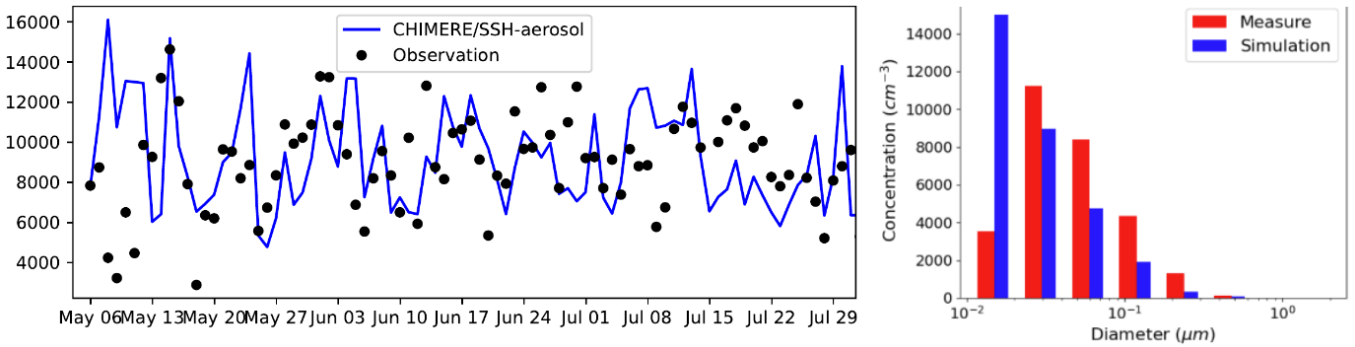

Figure 10. *Model to data comparison of N_{10} concentrations simulated over Madrid, Spain. The left panel illustrates the total N_{10} temporal evolution and the right panel the number concentration per size section [in cm^{-3}].*

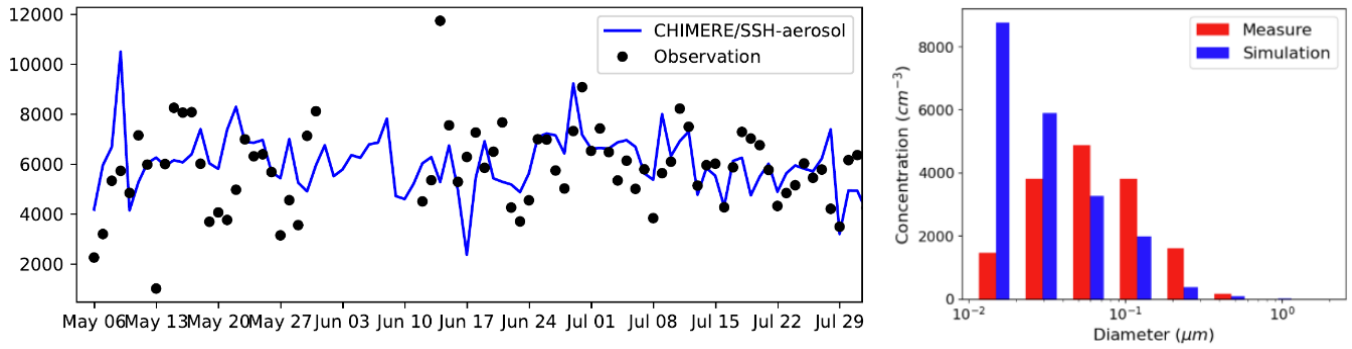

Figure 11. *Model to data comparison of N_{10} concentrations simulated over Ispra, Italy. The left panel illustrates the total N_{10} temporal evolution and the right panel the number concentration per size section [in cm^{-3}].*

Table 1 summarises the statistical indicators obtained at Barcelona, Madrid and Ispra stations, with MFB corresponding to the mean fractional bias, MFE corresponding to the mean fractional error and FAC2 the fraction of modelled data within a factor of 2 of observations. Daily simulated concentrations obtained with CHIMERE/SSH-aerosol are particularly close to observations in these stations, highlighting the strengths of this approach for urban background stations.

Table 1. *Statistical indicators obtained in the different stations for N_{10} model to data comparisons. MFB (%) and MFE (%) stand for Mean Fractional Bias and Mean Fractional Error respectively, FAC2 is FAC2 the fraction of modelled data within a factor of 2 of observations and Corr is the Correlation (in %).*

Station	Aver. Sim.	Aver. Obs.	MFB (%)	MFE (%)	FAC2 (%)	Corr. (%)
Barcelona	11 153	11 820	-8	25	96	50
Madrid	9233	8970	3	27	93	10
Ispra	6057	5798	7	24	96	14
All	8814	8863	1	25	95	25

5. SOURCE CONTRIBUTIONS ESTIMATIONS IN PMCAMx-UF

5.1 Source apportionment approach

Performing number source apportionment in a chemical transport model is challenging. Zeroing all but one source's number emissions results in changes of the condensation and coagulation sinks, to which

the model responds non-linearly for particle number concentrations. For that reason, in this work the Posner and Pandis (2015) approach is employed. This zero-out method eliminates emissions from specific sources below a certain diameter threshold. This approach allows us to retain most of the surface area and mass of the emitted particles while still capturing the source's contribution to the total number of emissions. The threshold diameter for each source is chosen to eliminate approximately 90% of its emissions (Table 2).

Table 2. *Zero-out diameters used for source apportionment simulations.*

Categories	Diameter (nm)	(%)
Public Power and Industry	81-102	88
Other stationary combustion/ Residential wood burning	129-162	89
On-road Gasoline	51-65	89
On-road Diesel	102-129	90
Shipping	41-51	90
Off-road	81-102	89
Aviation	65-81	90
Others (Fugitives, solvents, waste, etc.)	162-205	88

5.2 Source contribution predictions

The contributions of each source to the particle number (with high size resolution) have been estimated first at the European scale using 36×36 km^2 grid size simulations for the summer and winter of 2019. The sources examined in this work are as follows: nucleation, industry including power generation, small combustion, gasoline road transport, diesel road transport, shipping, off-road vehicles, other sources (fugitives, LPG road transport, non-exhaust road transport, waste, agricultural sources), and biomass burning. Figure 12 demonstrates that the major particle number contributor in Europe for summer is nucleation. While, for winter in Figure 13, for central Europe major particle number contributors are diesel and combustion. For north-eastern Europe, industry has the greatest impact on the particle number, while Mediterranean regions are most affected by nucleation.

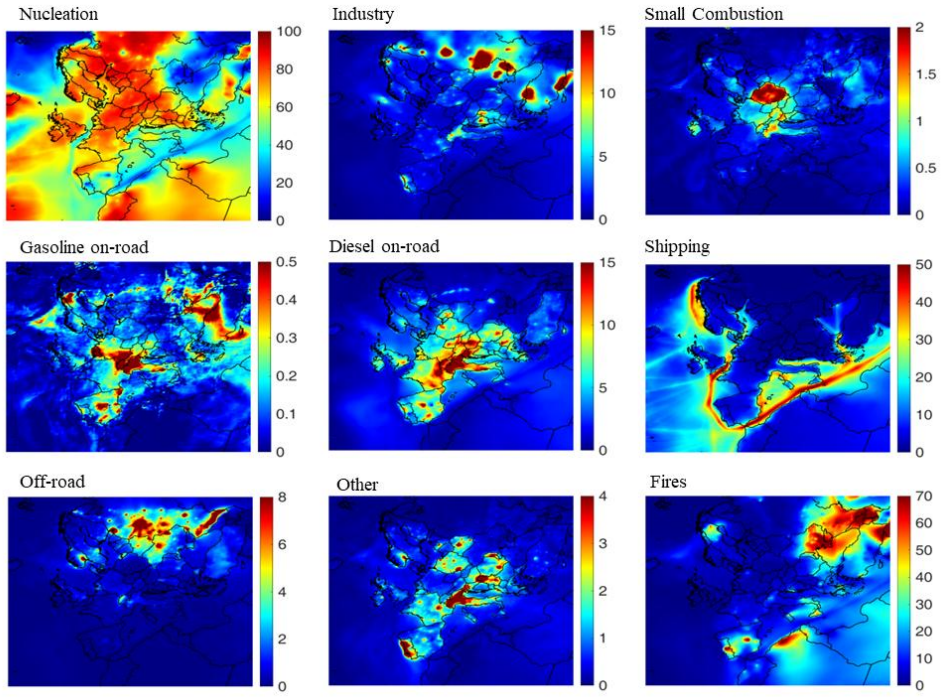

Figure 12. *Predicted source contributions as percentage of the total N_{10} over Europe for the summer of 2019 using PMCAMx-UF.*

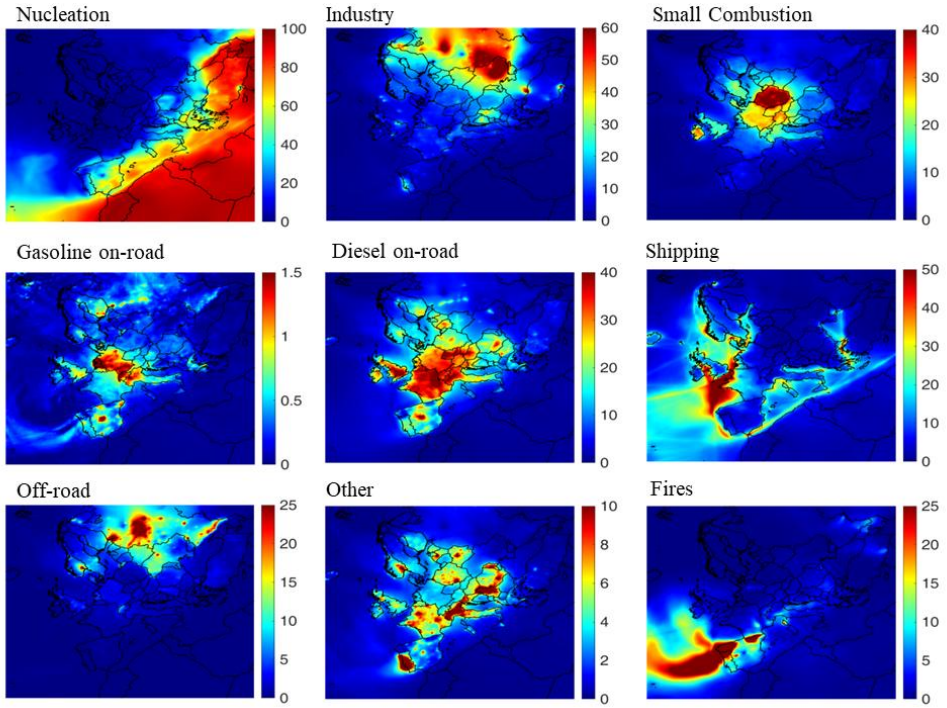

Figure 13. *Predicted source contributions as percentage of the total N_{10} over Europe for the winter of 2019 using PMCAMx-UF.*

5.3 Example for the case of Athens

Figure 14 displays the average particle number concentration over Athens for summer 2019 and winter 2019. For summer, high concentrations of particles are mainly found over the port of Piraeus and the Saronic gulf. While for winter, high particle concentrations are predicted over most of Athens.

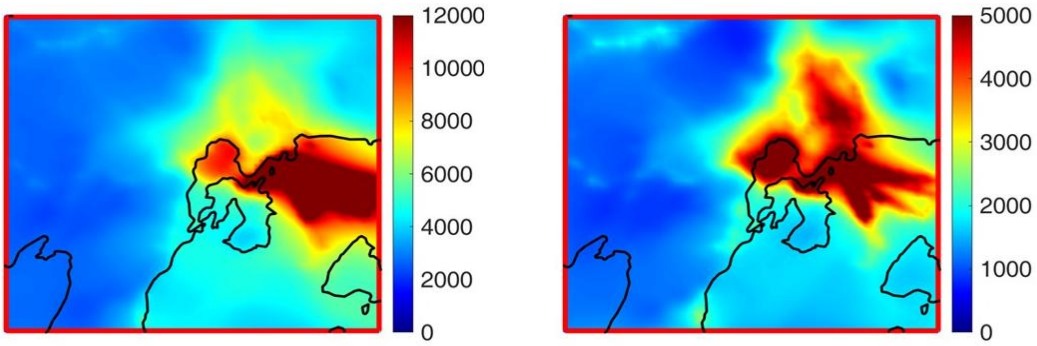

Figure 14. *Predicted ground-level N_{10} concentrations for the city of Athens for (left) summer of 2019 and (right) winter of 2019.*

Comparing the predictions of PMCAMx-UF using a 1×1 km^2 grid size against the observations from Demokritos, we notice that the model performs well for most of July, with a few days overestimating the number concentration (Figure 15). For the month of January, the model underpredicts the number concentration for most days (Figure 16). Errors in meteorology or underprediction of emissions (traffic, wood burning, other sources) could be responsible for this discrepancy.

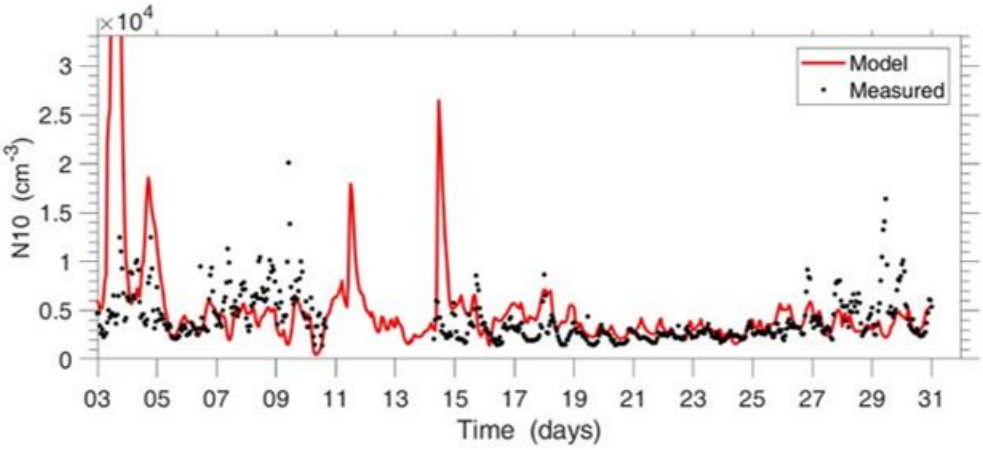

Figure 15. *Comparison of the measured N_{10} concentration in Demokritos with the predictions of PMCAMx-UF at high grid resolution for July 2019.*

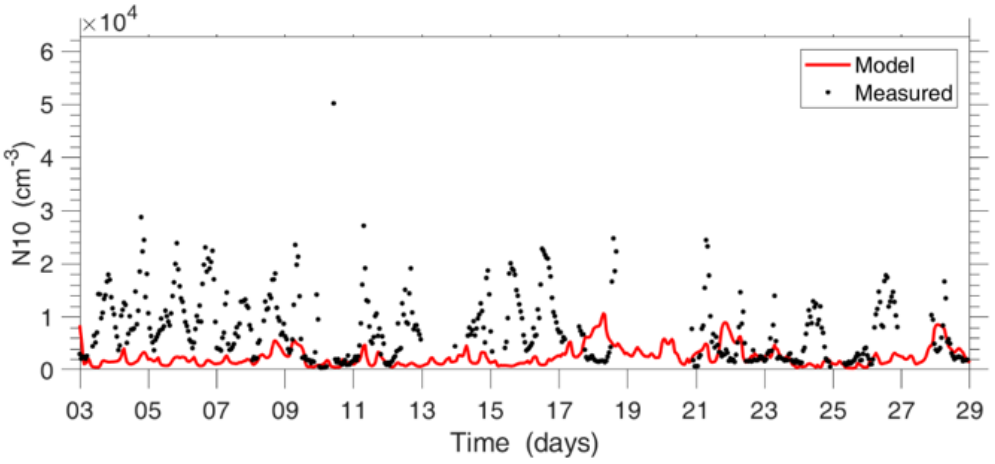

Figure 16. *Comparison of the measured N_{10} concentration in Demokritos with the predictions of PMCAMx-UF at high grid resolution for January 2019.*

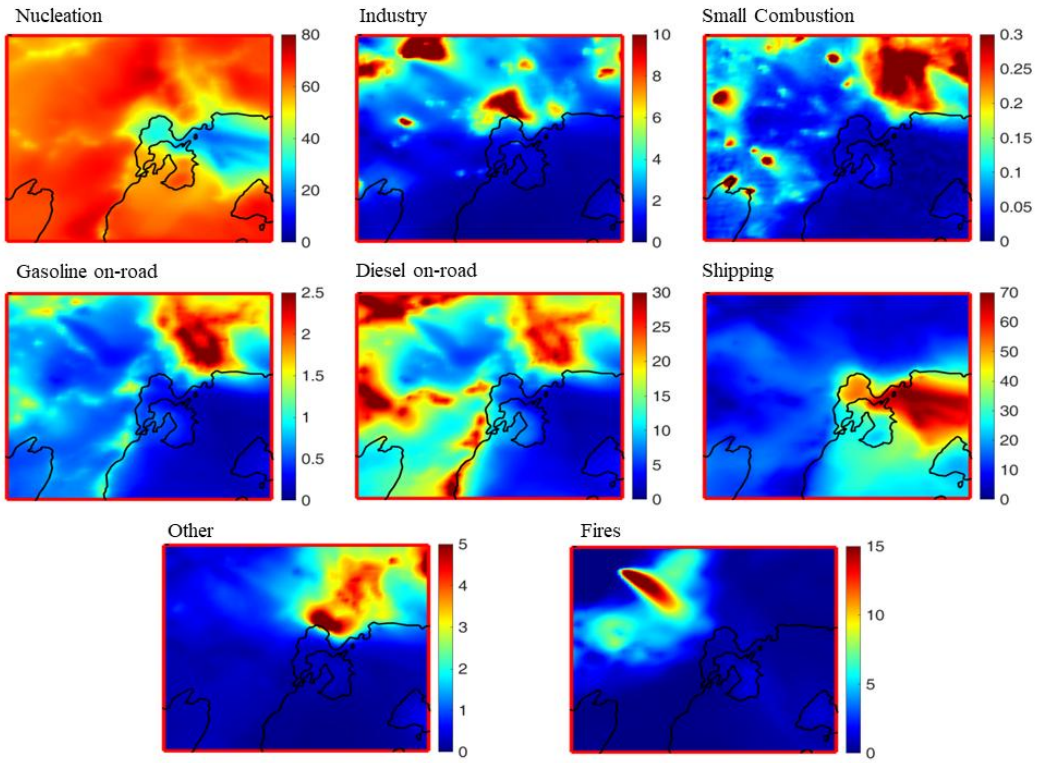

Figure 17*. Predicted source contributions as percentage of the total N10 over Athens for the summer of 2019 using PMCAMx-UF.*

Figure 17 displays the source contribution percentages over Athens for the summer. The major contributor to particle number concentration is nucleation for the whole modeling domain, diesel also has an important impact in the city center, and shipping has a great effect on the number concentration on the coast of Athens.

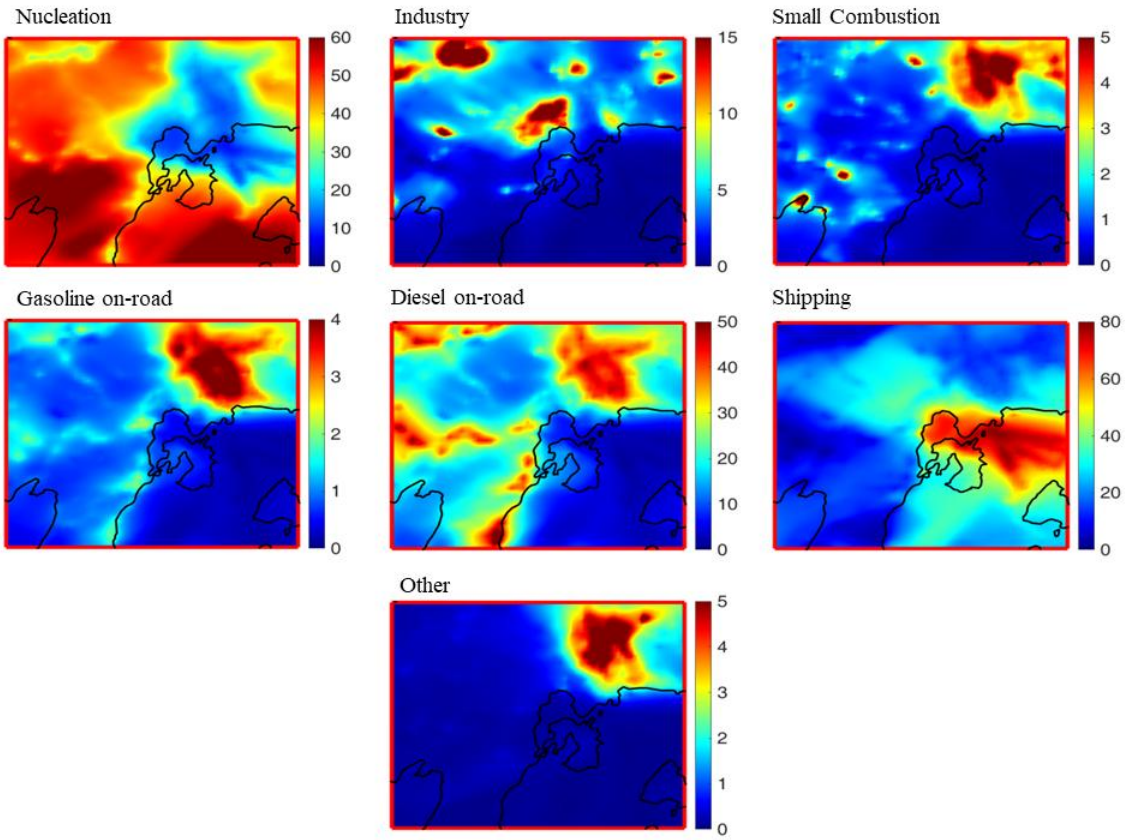

***Figure 18**. Predicted source contributions as percentage of the total N10 over Athens for the winter of 2019 using PMCAMx-UF.*

Figure 18 demonstrates the source contribution percentages over Athens for winter. Nucleation seems to dominate in most of the modeling domain with a much lower impact on the city center though. Diesel and shipping seem to be the main particle contributors for Athens.

6. Multi-scale simulations down to the street scale in CHIMERE/MUNICH/SSH-aerosol

6.1 Urban modelling

The concentrations of some pollutants, such as nitrogen dioxide (NO_2), $PM_{2.5}$, black carbon and the number of particles, are often observed to be particularly high over cities, with strong urban heterogeneities. In cities, particle number concentrations are particularly high along traffic axes and in streets. To estimate the outdoor concentrations to which populations are exposed, maps are required at spatial scales below 100 m, at the minimum, to be able to differentiate the street from the urban background concentrations. Hourly time resolution is desirable.

As detailed in the service tool "DETERMINISTIC URBAN MODELLING: PM & PN", local-scale modelling over cities is particularly suitable for representing the concentrations of pollutants that are highly influenced by urban heterogeneity. The multi-scale Eulerian model CHIMERE/MUNICH/SSH-aerosol (3-dimensional (3-D) Eulerian CTM grid model with sub-grid Eulerian dispersion and chemistry/aerosol dynamic at all scales) allows to tackle the variabilities of particle number and ultrafine particles down to the street scale.

6.2 CHIMERE/MUNICH/SSH-aerosol: example for the case of Paris

Multi-scale simulations are performed with the CHIMERE/MUNICH/SSH-aerosol modelling chain using nested domains down to the streets of Paris city for the winter 2020/2021 and the summer 2022. The modelling chain is presented and evaluated by comparisons to measurements of NO_2, $PM_{2.5}$, eBC and N_{10} in the service tool "DETERMINISTIC URBAN MODELLING: PM & PN". To gain computational time, only 10 sections between 10 nm and 10 µm are used, and nucleation is ignored. Simulations are performed with the bottom-up inventory Airparif (Parisian air quality agency) and the top-down inventory EMEP. As shown in Table 3, the modelled concentrations compare well to the measurements, satisfying the strictest criteria available in the literature (Boylan and Russell, 2006), which are met when the Mean Fractional Error is lower than 50% and the Mean Fractional Bias is lower than 30%. The FAC2 statistic is also evaluated. It is the fraction of modelled data within a factor of 2 of observations. It should be higher than 50% for the strictest criteria and 30% for a less strict criteria (Hanna and Chang 2012). Here it is always higher than 79%.

Table 3. *N_{10} model to measurement comparisons at urban background stations for summer and winter. MFB (%) and MFE (%) stand for Mean Fractional Bias and Mean Fractional Error respectively, FAC2 is FAC2 the fraction of modelled data within a factor of 2 of observations.*

Period	Number of stations	Aver. Obs. (# cm^{-3})	Emission inventory	Aver. Sim. (# cm^{-3})	MFE (%)	MFB (%)	FAC2 (%)	Corr. (%)
Summer	4	8176	Airparif	8173	25	4	98	59
			EMEP	10611	35	27	89	44
Winter	5	7091	Airparif	8025	43	22	79	49
			EMEP	10112	48	32	81	36

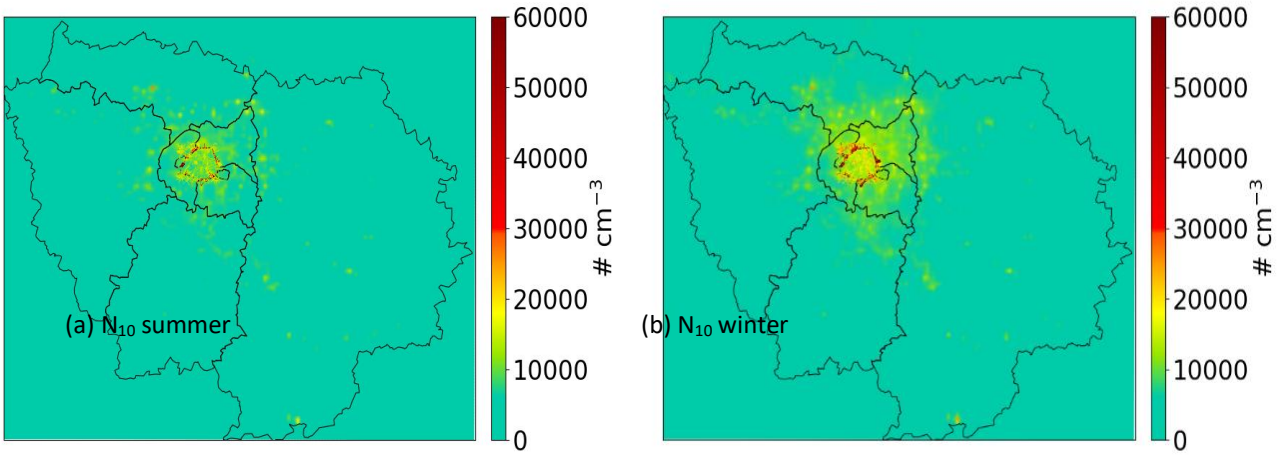

Figure 19. *N_{10} concentrations (in # cm^{-3}) simulated for summer (left panels) and winter (right panels) using CHIMERE/MUNICH over the Greater Paris area.*

Figure 19 shows the N_{10} concentrations over Paris during summer and winter, stressing the large urban heterogeneities that are observed for number concentrations.

The size distribution of the number concentrations is also very well modelled, both in summer and winter, as shown in Figure 20 for summer and Figure 21 for winter. In the model as in the observations, the concentrations are much larger at the station in the city center (PA01H, Châtelet les Halles) than at the suburban or rural station (suburban SIRTA for the summer comparison, and rural station in the south of the Greater Paris for the winter comparison).

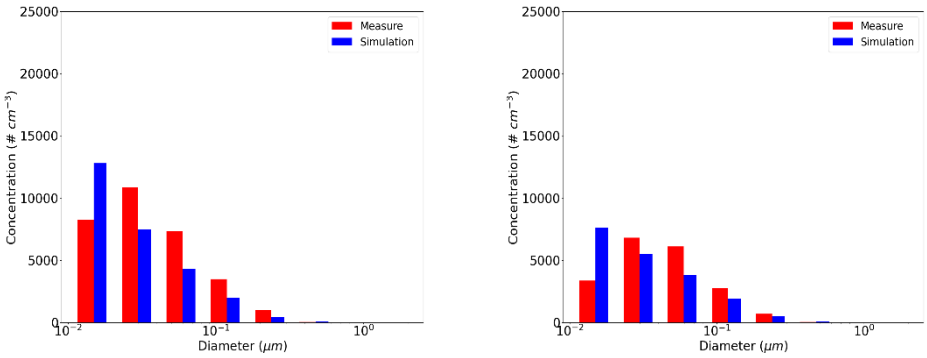

Figure 20. *Number concentrations (in # cm^{-3}) simulated for summer at a Airparif station in the city center (PA01H, left panel) and a suburban station (SIRTA, right panels).*

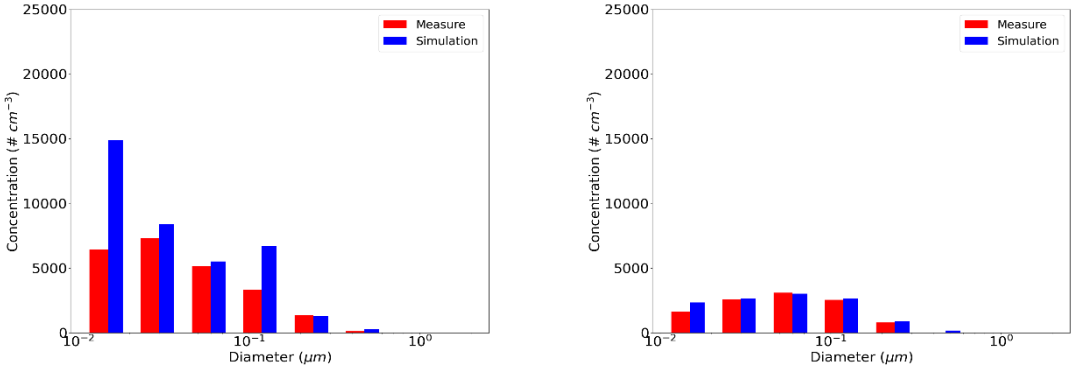

Figure 21. *Number concentrations (in cm^{-3}) simulated for winter at a station in the city center (PA01H, left panel) and a rural station south of Greater Paris (right panel).*

7. RECOMMENDATIONS IN CASE STAKEHOLDERS HAVE TO START NOW TO IMPLEMENT IMPLEMENT MODEL

3D air-quality modelling may be used to represent the spatio-temporal variations of UFP and number concentrations. Chemical transport models, such as PMCAMx-UF or CHIMERE/MUNICH/SSH-aerosol may be used. They need to model complex physical-chemical processes including coagulation, condensation of semi and low-volatile chemical compounds and/or nucleation processes.

To ensure the successful implementation of either PMCAMx-UF or the CHIMERE/MUNICH/SSH-aerosol model chain, stakeholders must adhere to specific steps and fulfill the model's requirements.

First and foremost, it is imperative to ensure that the technical infrastructure is adequate, encompassing sufficient computational power and storage capacity to meet the model's demands. It is recommended that the system possesses a minimum of 8 GB of RAM. Given the computationally intensive nature of PMCAMx-UF and CHIMERE/MUNICH/SSH-aerosol, it necessitates robust resources such as supercomputers or cloud computing infrastructure capable of managing large data volumes and intricate computational processes. Additionally, storage capacity must be ample to accommodate daily output volumes of approximately 4 GB.

Secondly, it is essential to gather and process the requisite input data, which includes comprehensive meteorological data, emissions data, and information on local pollution sources. Specifically, for street-level simulations with MUNICH, traffic emissions per street are required. Detailed and precise meteorological data are crucial for input into the model, encompassing parameters such as temperature, humidity, wind speed and direction, and solar radiation. Additionally, emissions data from various sources—including industrial facilities, vehicular traffic, agricultural activities, and natural sources—must be collected, detailing both the quantities and chemical compositions of the emissions. To ensure the reliability and accuracy of this data, rigorous data cleaning and verification processes should be employed.

Facilitate training sessions for personnel designated to operate PMCAMx-UF and/or CHIMERE/MUNICH/SSH-aerosol, led by experts from the development teams (LAQS team at the FORTH Institute for PMCAMx-UF and CEREA laboratory for CHIMERE/MUNICH/SSH-aerosol). This training should include the provision of educational materials and detailed information explaining the operation, capabilities, and best practices of the model. Proficiency in atmospheric chemistry and meteorology is

essential, along with strong skills in data management and analysis, to ensure effective utilization of the models. Additionally, future stakeholders should possess expertise in computational languages such as FORTRAN, Python, or R. The user must possess the capability to handle and analyze Weather Research and Forecasting (WRF) data, which will serve as input information for the model. Additionally, proficiency in installing essential libraries, such as the Intel Fortran Compiler (ifort), is required. Understanding the installation and configuration of these libraries is crucial for ensuring the model operates correctly and efficiently on the computational infrastructure. This expertise is essential for maintaining the integrity and performance of the modeling processes.

Additionally, the models should be integrated into existing air quality monitoring and management processes, with adaptations made to suit local conditions and requirements. This integration may necessitate collaboration with local authorities and scientific organizations to ensure the acquisition and analysis of pertinent data, as well as the incorporation of the models into current monitoring systems. Clear performance indicators should be established to evaluate the model's effectiveness, and a feedback mechanism should be created for continuous improvement and adaptation of the model. Pilot applications of the models should be planned in specific regions to conduct initial performance assessments and identify any potential issues or limitations.

Finally, collaboration and support from all stakeholders, including local authorities, scientific organizations, and the community, should be ensured to enhance the successful implementation of PMCAMx-UF and/or CHIMERE/MUNICH/SSH-aerosol. The benefits and capabilities of the models should be communicated through informational meetings and reports to secure commitment and active participation from all involved parties. Continuous updates and upgrades to the model and its databases should be performed to ensure the accuracy and reliability of the results. By following these steps and meeting the requirements, stakeholders can ensure the effective and efficient use of the models, enhancing its value and contribution to operational processes.

8. GROUP TO BE CONTACTED TO HELP WITH THE TOOL IMPLEMENTATION

PMCAMx-UF

Laboratory of Air Quality Studies (LAQS):

- Spyros N. Pandis: *spyros@chemeng.upatras.gr*
- David Patoulias: *davidpat@chemeng.upatras.gr*
- Elena Poulikidi: *up1069028@upnet.gr*
- Evangelia Siouti: *siouti.valia@chemeng.upatras.gr*
- Ksakousti Skyllakou: *ksakousti@chemeng.upatras.gr*

CHIMERE/MUNICH/SSH-aerosol

CEREA Laboratory:

- Karine Sartelet: *karine.sartelet@enpc.fr*
- Lya Lugon: *lya.lugon@enpc.fr*
- Youngseob Kim: *youngseob.kim@enpc.fr*
- Yelva Roustan: *yelva.roustan@enpc.fr*

LMD Laboratory*:*

- *Myrto Valari: myrto.valari@lmd.ipsl.fr*

9. REFERENCES

Carter, W.P., 2007. A detailed mechanism for the gas-phase atmospheric reactions of organic compounds. Atmos. Environ., 41, 80-117, https://doi.org/10.1016/j.atmosenv.2007.10.061

Chrit, M., Sartelet, K., Sciare, J., Pey, J., Marchand, N., Couvidat, F., Sellegri, K. and Beekmann, M., 2017. Modelling organic aerosol concentrations and properties during ChArMEx summer campaigns of 2012 and 2013 in the western Mediterranean region. Atmos. Chem. Phys., 17, 12509-12531, https://doi.org/10.5194/acp-17-12509-2017

Couvidat, F. and Sartelet, K., 2015. The Secondary Organic Aerosol Processor (SOAP) model: a unified model with different ranges of complexity based on the molecular surrogate approach. Geosci. Model Dev., 8, 1111-1138, https://doi.org/10.5194/gmd-8-1111-2015

Derognat, C., Beekmann, M., Baeumle, M., Martin, D., and Schmidt, H., 2003. Effect of biogenic volatile organic compound emissions on tropospheric chemistry during the Atmospheric Pollution Over the Paris Area (ESQUIF) campaign in the Ile-de-France region. J. Geophys. Res., 108, 8560, https://doi.org/10.1029/2001jd001421

Devilliers, M., Debry, E., Sartelet, K., Seigneur, C., 2013. A new algorithm to solve condensation/evaporation for ultra fine, fine, and coarse particles. J. Atmos. Sci., 55, 116-136, https://doi.org/10.1016/j.jaerosci.2012.08.005

Fountoukis, C., Riipinen, I., Van Der Gon, H.D., Charalampidis, P.E., Pilinis, C., Wiedensohler, A., O'Dowd, C., Putaud, J.P., Moerman, M. and Pandis, S.N., 2012. Simulating ultrafine particle formation in Europe using a regional CTM: contribution of primary emissions versus secondary formation to aerosol number concentrations. Atmos. Chem. Phys., 12, 8663–8677, https://doi.org/10.5194/acp-12-8663-2012

Gaydos, T.M., Stainer, C.O. and Pandis, S.N., 2005. Modeling of in situ ultrafine atmospheric particle formation in the eastern United State. J. Geophys. Res., 110, D07S12, https://doi.org/10.1029/2004JD004683

Grythe, H., Ström, J., Krejci, R., Quinn, P. and Stohl, A., 2014. A review of sea-spray aerosol source functions using a large global set of sea salt aerosol concentration measurements. Atmos. Chem. Phys., 14, 1277-1297, https://doi.org/10.5194/acp-14-1277-2014

Guenther, A., Karl, T., Harley, P., Wiedinmyer, C., Palmer, P.I., Geron, C., 2006. Estimates of global terrestrial isoprene emissions using MEGAN (Model of Emissions of Gases and Aerosols from Nature). Atmos. Chem. Phys., 6, 3181–3210, https://doi.org/10.5194/acp-6-3181-2006

Guenther, A.B., Jiang, X., Heald, C.L., Sakulyanontvittaya, T., Duhl, T., Emmons, L.K., Wang, X., 2012. The Model of Emissions of Gases and Aerosols from Nature version 2.1 (MEGAN2.1): An extended and

updated framework for modeling biogenic emissions. Geosci. Model Dev., 5, 1471–1492, https://doi.org/10.5194/gmd-5-1471-2012

Hanna, S. ans Chang, J., 2012. Acceptance criteria for urban dispersion model evaluation. Meteorol. Atmos. Phys., 116, 133-146, https://doi.org/10.1007/s00703-011-0177-1

Hopke, P.K., Feng, Y., Dai, Q., 2022. Source apportionment of particle number concentrations: A global review. Sci. Total Environ. 819, 153104. https://doi.org/10.1016/j.scitotenv.2022.153104

Jacquot, O. and Sartelet, K., 2024. Numerical investigations on the modelling of ultrafine particles in SSH-aerosol-v1.3a: size resolution and redistribution, Geosci. Model Dev. Discuss., https://doi.org/10.5194/gmd-2024-150

Jung, J.G., Fountoukis, C., Adams, P.J. and Pandis, S.N., 2010. Simulation of in situ ultrafine particle formation in the eastern United States using PMCAMx-UF. J. Geophys. Res., 115, D03203, https://doi.org/10.1029/2009JD012313

Jung, J.G., P.J. Adams and S.N. Pandis, 2008. Evaluation of nucleation theories in a sulfur-rich environment. Aerosol Sci. Tech., 42, 495-504, https://doi.org/10.1080/02786820802187085

Jung, J., Adams, P.J. and Pandis, S.N., 2006. Simulating the size distribution and chemical composition of ultrafine particles during nucleation events. Atmos.Environ., 40 (13), 2248–2259, https://doi.org/10.1016/j.atmosenv.2005.09.082

Kuenen, J., Dellaert, S., Visschedijk, A., Jalkanen, J.-P., Super, I., and Denier van der Gon, H., 2022. CAMS-REG-v4: a state-of-the-art high-resolution European emission inventory for air quality modelling. Earth Syst. Sci. Data, 14, 491–515, https://doi.org/10.5194/essd-14-491-2022

Kim, Y., Lugon, L., Maison, A., Sarica, T., Roustan, Y., Valari, M., et al., 2022. MUNICH v2. 0: a street-network model coupled with SSH-aerosol (v1.2) for multi-pollutant modelling. Geosci. Model Dev., 15 (9), 7371-7396, https://doi.org/10.5194/gmd-15-7371-2022

Kuang, C., McMurry, P., McCormick, A. and Eisele, F., 2008. Dependence of nucleation rates on sulfuric acid vapor concentration in diverse atmospheric locations. J. Geophys. Res., 113, D10209, https://doi.org/10.1029/2007JD009253

Maison A., Lugon L., Park S.-J., Boissard C., Faucheux A., Gros V., Kalalian C., Kim Y., Leymarie J., Petit J.-E., Roustan Y., Sanchez O., Squarcioni A., Valari M., Viatte C., Vigneron J., Tuzet A., Sartelet K., 2024. Contrasting effects of urban trees on air quality: From the aerodynamic effects in streets to impacts of biogenic emissions in cities. Sci. Tot. Environ., 946, 174116, https://doi.org/10.1016/j.scitotenv.2024.174116

Martensson, E.M., Nilsson, E.D., de Leeuw, G., Cohen, L.H., and Hansson, H.-C., 2003. Laboratory simulations and parameterization of the primary marine aerosol production. J. Geophys. Res. - Atmos, 108 (D09), 4297, https://doi.org/10.1029/2002JD002263

Menut, L., Bessagnet, B., Briant, R., Cholakian, A., Couvidat, F., Mailler, S., et al., 2021. The CHIMERE v2020r1 online chemistry-transport model. Geosci. Model Dev, 14 (11), 6781-6811, https://doi.org/10.5194/gmd-14-6781-2021

Menut, L., Cholakian, A., Siour, G., Lapere, R., Pennel, R., Mailler, S., and Bessagnet, B.: Impact of Landes forest fires on air quality in France during the 2022 summer, 2023. Atmos. Chem. Phys., 23, 7281–7296, https://doi.org/10.5194/acp-23-7281-2023

Monahan, E.C., Spiel, D.E., Davidson, K.L. (1986). A Model of Marine Aerosol Generation Via Whitecaps and Wave Disruption. In: Monahan, E.C., Niocaill, G.M. (eds) Oceanic Whitecaps. Oceanographic Sciences Library, vol 2, pp.167-174. Springer, Dordrecht. https://doi.org/10.1007/978-94-009-4668-2_16

Napari, I., Noppel, M., Vehkamäki, H. and Kulmala, M., 2002. Parameterization of ternary nucleation rates for H_2SO_4-NH_3-H_2O Vapors. J. Geophys. Res. - Atmos, 107 (D19), 4381–4386, https://doi.org/10.1029/2002JD002132

O'Dowd, C.D., Langmann, B., Varghese, S., Scannell, C., Ceburnis, D., Facchini, M.C., 2008. A combined organic-inorganic sea-spray source function. Geophys. Res. Lett., 35, L01801, https://doi.org/10.1029/2007GL030331

Olin, M., Patoulias, D., Kuuluvainen, H., Niemi, J.V., Rönkkö, T., Pandis, S.N., et al., 2022. Contribution of traffic-originated nanoparticle emissions to regional and local aerosol levels. Atmos. Chem. Phys., 22 (2), 1131-1148, https://doi.org/10.5194/acp-22-1131-2022

Park, S., Lugon L., Jacquot, O., Kim, Y., Baudic A., D'Anna, B., Di Antonio, L., Di Biagio, C., Dugay F., Favez, O., Ghersi, V., Gratien, A., Kammer, J., Petit, J-E., Sanchez, O., Valari, M., Vigneron, J., and Sartelet, K., 2024. Population exposure to outdoor NO_2, black carbon, particle mass, and number concentrations over Paris with multi-scale modelling down to the street scale. Atmos. Chem. Phys., in review. Preprint: https://doi.org/10.5194/egusphere-2024-2120

Patoulias, D. And Pandis, S.N., 2022. Simulation of the effects of low-volatility organic compounds on aerosol number concentrations in Europe. Atmos. Chem. Phys., 22, 1689–1706, https://doi.org/10.5194/acp-22-1689-2022

Patoulias, D., Fountoukis, C., Riipinen, I. and Pandis, S.N., 2015. The role of organic condensation on ultrafine particle growth during nucleation events. Atmos. Chem. Phys., 15, 6337–6350, https://doi.org/10.5*194/acp-15-6337-2015

Pierce, J.R. and Adams, P.J., 2009. Uncertainty in global CCN concentrations from uncertain aerosol nucleation and primary emission rates. Atmos. Chem. Phys., 9, 1339–1356, https://doi.org/10.5194/acp-9-1339-2009

Posner, L.N. and Pandis, S.N., 2015. Sources of ultrafine particles in the Eastern United States. Atmos. Environ., 111, 103–112, https://doi.org/10.1016/j.atmosenv.2015.03.033

Riccobono, F., Schobesberger, S., Scott, C., Dommen, J., Ortega, I., Rondo, L., Almeida, J., Amorim, A., Bianchi, F., Breitenlechner, M., David, A., et al., 2014. Oxidation products of biogenic emissions contribute to nucleation of atmospheric particles. Science, 16, 717–721, https://doi.org/10.1126/science.1243527

Sartelet, K., Kim, Y., Couvidat, F., Merkel, M., Petäjä, T., Sciare, J. and Wiedensohler, A., 2022. Influence of emission size distribution and nucleation on number concentrations over Greater Paris. Atmos. Chem. Phys., 22, 8579-8596, https://doi.org/10.5194/acp-22-8579-2022

Sartelet, K., Couvidat, F., Wang, Z., Flageul, C., Kim, Y., 2020. SSH-aerosol v1. 1: A modular box model to simulate the evolution of primary and secondary aerosols. Atmosphere, 11 (5), 525, https://doi.org/10.3390/atmos11050525

Skamarock, W.C., Klemp, J.B., Dudhia, J., Gill, D.O., Barker, D.M., Duda, M.G., et al., 2008. A description of the advanced research WRF version 3. NCAR technical note, 475(125), 10-5065, https://doi.org/10.5065/D68S4MVH

Ramacher, M.O.P., Kakouri, A., Speyer, O., Feldner, J., Karl, M., Timmermans, R., Denier van der Gon, H., Kuenen, J., Gerasopoulos, E., Athanasopoulou, E., 2021. The UrbEm hybrid method to derive high-resolution emissions for city-scale air quality modeling. Atmosphere, 12, 1404, https://doi.org/10.3390/atmos12111404

Skamarock, W.C., Klemp, J.B., Dudhia, J., Gill, D.O., Liu, Z., Berner, J., Wang, W., Powers, J.G., Duda, M.G., Barker, D.M., et al. A description of the Advanced Research WRF Model Version 4.1; No. NCAR/TN-556+STR; National Center for Atmospheric Research: Boulder, CO, USA, 20 July 2021.

Trechera, P., Garcia-Marlès, M., Liu, X., Reche, C., Pérez, N., Savadkoohi, et al., 2023. Phenomenology of ultrafine particle concentrations and size distribution across urban europe. Environ. Int., 172, 107744, https://doi.org/10.1016/j.envint.2023.107744

Vehkamäki, H., Kulmala, M., Napari, I., Lehtinen, K.E.J., Timmreck, C., Noppel, M., Laaksonen, A., 2002. An improved parameterizationfor sulfuric acid–water nucleation rates for tropospheric and stratospheric conditions. J. Geophys. Res., 107, 4622, https://doi.org/10.1029/2002JD002184

Spada, M., Jorba, O., Pérez García-Pando, C., Janjic, Z. and Baldasano, J., 2013. Modeling and evaluation of the global sea-salt aerosol distribution: sensitivity to size-resolved and sea-surface temperature dependent emission schemes. Atmos. Chem. Phys., 13 (23), 11735-11755, https://doi.org/10.5194/acp-13-11735-2013

Van Leer, B., 1977. Towards the ultimate conservative difference scheme. IV. A new approach to numerical convection. J. Comput. Phys., 23 (3), 276-299, https://doi.org/10.1016/0021-9991(77)90095-X

Wesely, M.L., 1967. Parameterization of surface resistances to gaseous dry deposition in regional-scale numerical models. Atmos. Environ., 23 (6), 52-63, https://doi.org/10.1016/0004-6981(89)90153-4